Journal of Magnetism and Magnetic Materials 324 (2012) 2158–2162

Contents lists available at SciVerse ScienceDirect

Journal of Magnetism and Magnetic Materials

journal homepage: www.elsevier.com/locate/jmmm

Effect of annealing on phase composition, structural and magnetic properties of Sm-Co based nanomagnetic material synthesized by sol-gel process

G. Suresh [a], P. Saravanan [b], D. Rajan Babu [a,*]

[a] Advanced Materials Research Centre, School of Advanced Sciences, VIT University, Vellore 632 014, India
[b] Defence Metallurgical Research Laboratory, Hyderabad 500 058, India

ARTICLE INFO

Article history:
Received 1 September 2011
Received in revised form
1 February 2012
Available online 28 February 2012

Keywords:
Chemical synthesis
Sol-gel process
Samarium cobalt
Magnetic nanoparticle

ABSTRACT

Sm-Co based nanomagnetic material was synthesized by means of a Pechini-type sol-gel process. In this method, a suitable gel-precursor was prepared using respective metal salts and complexing agent such as citric acid. The gel-precursor was dried at 300 °C and then subjected to various reductive annealing temperatures: 350, 500 and 600 °C. The nanopowders so obtained were characterized for their structure, phase composition and magnetic properties. FT-IR studies on the gel-precursor showed the binding of metal cations with the citrate molecules in the form of metal-citrate complex. The gel-precursor, which was annealed at 350 °C showed the presence of both meta-stable cobalt carbide (Co_2C, Co_3C) and Co_3O_4 phases; while the sample annealed at 500 °C indicated the sign of $SmCo_5$ phase. Upon increasing the reductive annealing temperature to 600 °C, crystalline phase such as fcc-Co and Sm_2C_3 were formed prominently. FE-SEM analysis revealed the change in sample morphology from spherical to oblate spheres upon increasing the annealing temperature. VSM measurements demonstrated ferromagnetic nature at room temperature for all the nanopowders obtained irrespective of their after reductive annealing temperature.

1. Introduction

Among the rare-earth permanent magnets, the highly anisotropic Sm-Co compounds such as $SmCo_5$, $SmCo_7$, Sm_2Co_{17}, and Sm_5Co_{19} are technologically important on account of their intrinsic magnetic properties. Of all the Sm-Co intermetallic compounds, $SmCo_5$ and Sm_2Co_{17} are the two important hard magnetic phases [1] and they crystallize in hexagonal $CaCu_5$ and Th_2Ni_{17} or rhombohedral-Th_2Zn_{17} structure, respectively [2,3]. Both these magnetic phases have been extensively investigated in the past decades for their applications as permanent magnets at elevated temperatures; in particular, $SmCo_5$ is widely known for its intrinsic characteristics such as high magneto-crystalline anisotropy and high Curie temperature [3–5]. In view of the perceived advantages of Sm-Co compounds in their bulk form; in recent years, considerable efforts have been made on the synthesis of nanomagnetic materials of Sm-Co compounds utilizing a variety of conventional processing routes, viz., ball-milling [6], thermal decomposition [5], reductive annealing [7], polyol process [8,9], spin coating [10] and superhydride reduction [11]. Very recently, Harris et al. reported that the wet-chemical synthesis of Sm-Co nanoparticles through polyol process, which resulted in Co_2C, Co_3C and Sm-Co phases [12]. As the X-ray diffraction patterns of Sm-Co, Co_2C and Co_3C phases are quite similar, the identification of individual phase components was not realistic and led to misconception [12–14]. In the wet-chemical synthesis, the redox potential of the reducing reagent must be more negative than that of the metal ions which is an important factor in controlling the formation of Sm-Co phases. A stronger reducing reagent is supposed to be preferred for the reduction of metal ions having higher electronegativity [15]. As the oxidation potential of Sm and Co is (−2.301 V) and (−0.28 V) respectively [16], the co-reduction of both the metal ions should be attempted during the wet-chemical process, in order to achieve the required Sm-Co crystalline phase. In this context, Pechini-type sol-gel process is considered as one of the most successful routes for synthesizing metal alloy nanoparticles with required phase homogeneity, as compared to other wet-chemical methods such as polyol and co-precipitation. This technique caters the ability of organic acids for the formation of metal organic complexes [17]; upon suitable reductive annealing, these complexes transformed into respective alloy nanoparticles. Herein, we intend to employ such a process to synthesis Sm-Co based nanomagnets with a variety of crystalline phases by suitably controlling the reductive annealing temperature.

2. Materials and method

In order to prepare a thermally stable sol, 2 mmol of samarium acetate tetrahydrate, 10 mmol of cobalt acetate tetrahydrate, 16 mmol of citric acid and 16 mmol of ethylene glycol were

* Corresponding author. Tel.: +91 94434 71434; fax: +91 416 220 2804.
E-mail addresses: drajanbabu@vit.ac.in, rajanbabud@hotmail.com (D. Rajan Babu).

0304-8853/$ - see front matter © 2012 Elsevier B.V. All rights reserved.
doi:10.1016/j.jmmm.2012.02.038

dissolved in 50 ml of de-ionized water. The contents were heated to 80 °C with gentle stirring to form a highly viscous gel and subsequently the gel was allowed to dry at 300 °C in air and named as SMC-1. The powder samples of SMC-1 were further annealed at 350, 500 and 600 °C in H_2 atmosphere for 30 minutes and named as SMC-2, SMC-3 and SMC-4, respectively.

2.1. Characterizations

X-ray diffraction (XRD) patterns were recorded using Bruker D8 Advance diffractometer with Cu $K\alpha_1$ radiation ($\lambda = 1.5406$ Å) at a scanning speed of 0.005°/sec. Fourier transform infrared (FT-IR) spectra were recorded using a Nicolet Avator 330 spectrometer. Thermogravimetric analysis (TGA) was carried out at a rate of 10 °C/min in N_2 atmosphere using SDT Q600, TA Instrument, USA equipped with Thermal Advantage software. Field emission-scanning electron microscope (FE-SEM) imaging was carried out in FEI Quanta FEG 200 equipped with energy dispersive X-ray (EDX) spectrometer. The magnetic hysteresis measurements were carried out in room temperature using Lakeshore vibrating sample magnetometer (VSM) 7410 at a maximum applied field of 20 kOe.

3. Results and discussion

The synthesis of Sm-Co based nanomagnetic material using the Pechini-type sol-gel technique has two steps: (i) formation of metal-citrate gel precursor and (ii) annealing of the gel precursor at different temperatures: 350, 500 and 600 °C under H_2 atmosphere. Fig. 1 shows XRD patterns obtained for all the samples indicating the formation of various crystalline phases. Sharp diffraction peaks could be observed from the XRD pattern of SMC-1 and the observed peaks indicate the crystallization of Co_3O_4 phase (JCPDS card No. 042-1467); which is due to the drying of gel in ambient conditions. The gradual decomposition of Co_3O_4 phase was observed upon annealing the sample under H_2 atmosphere at different temperatures. Furthermore, the growth of other phases can be witnessed. Fig. 2(a) shows the XRD patterns of SMC-2 and SMC-3 and the XRD peaks appear to be broad, which may be due to the small crystallite size [18]. The analysis of XRD patterns revealed the presence of several other crystallographic phases such as $SmCo_5$, Co_2C, Co_3C, Co_3O_4 and CoO. The presence of $SmCo_5$ phase cannot be ruled out; though the XRD patterns of Co_2C and $SmCo_5$ are almost similar [12]. The SMC-2 has majority of Co_3C phase and minority of oxide phases. From the XRD pattern of sample SMC-3 (Fig. 2(a)), crystallization of $SmCo_5$ and partial crystallization of fcc-Co phase can be clearly noticed. The XRD pattern of Co_2C, Co_3C and $SmCo_5$ phases are consistent with that of their bulk with JCPDS card numbers: 065–1457, 043-1144 and 065–4157, respectively. From the XRD pattern of SMC-4 (Fig. 2 (b)), the presence of fcc-Co, Sm_2C_3, SmO and Co_3O_4 phases are witnessed with no evidence of $SmCo_5$ phase. The $SmCo_5$ phase, which is crystallized in SMC-3 has decomposed in SMC-4 due to the secondary phase crystallization of fcc-Co (JCPDS card No. 015-0806). The secondary crystallization of fcc-Co is generally observed in cobalt-based alloys, when the sample is subjected to annealing sufficiently higher temperature [19]. The decomposition of cobalt carbide phases is due to their

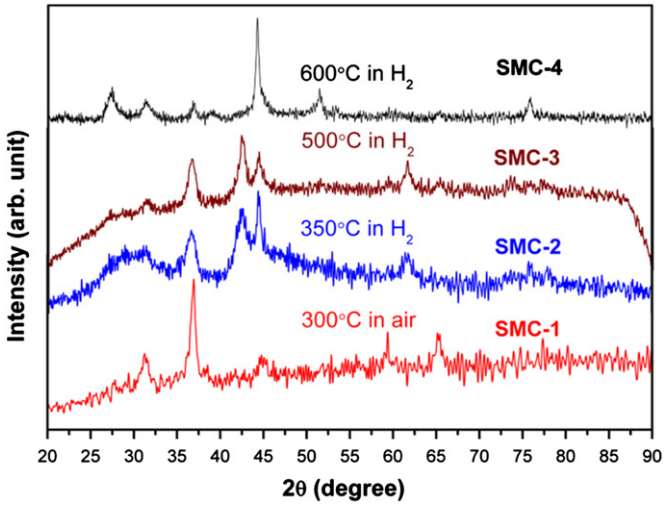

Fig. 1. XRD patterns of gel precursors subjected to different annealing temperatures.

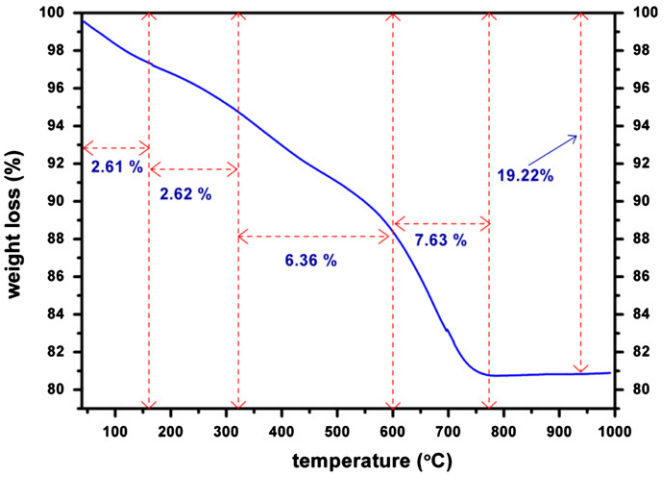

Fig. 3. TGA trace of SMC-1.

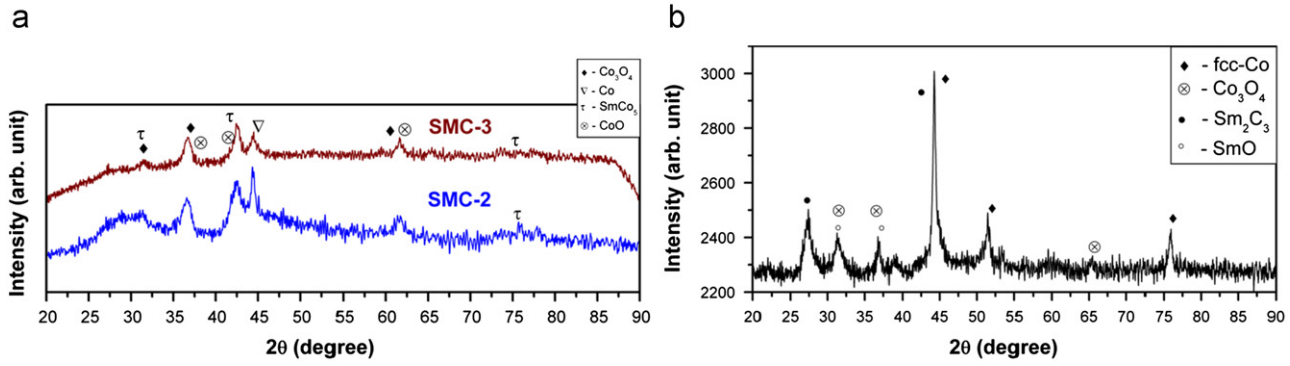

Fig. 2. (a) XRD patterns of SMC-2, SMC-3 and (b) XRD pattern of SMC-4.

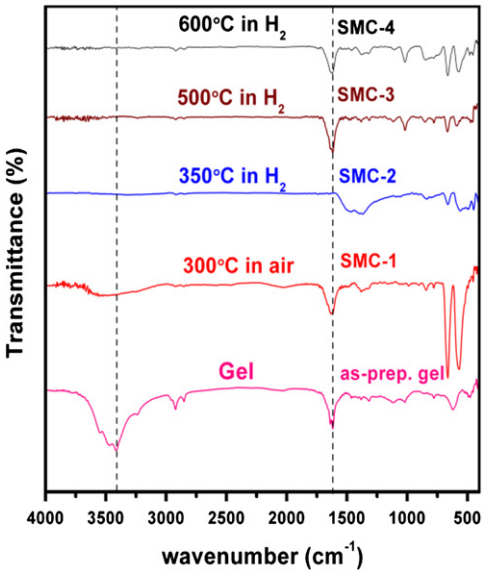

Fig. 4. FT-IR spectra of as-prepared gel precursor and its annealed counterparts at different temperatures.

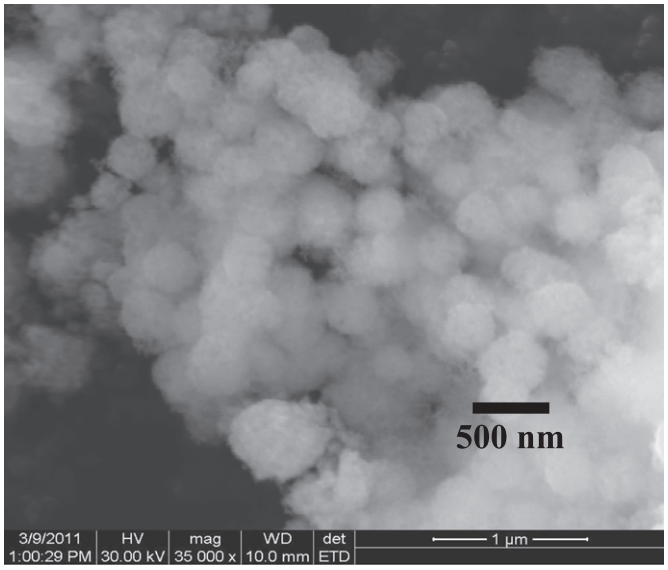

Fig. 5. (a) FE-SEM image of spherical granules of SMC-2.

meta-stable nature and these phases are generally stable up to 600 °C [20]. The peak observed at 27.5° reveals the presence of Sm_2C_3; while the peak noticed at 31.6° reveals the presence of SmO and Co_3O_4 phases.

The TGA trace of SMC-1 (Fig. 3) shows weight loss in four steps. The observed weight loss was gradual from room temperature to 160 °C (step-1), 160 to 320 °C (step-2), 320 to 600 °C (step-3) and 600 to 773 °C (step-4). The thermal decomposition of the metal citrate complex is the most important and the most complex stage [21]. The decomposition involves a few steps, which includes dehydration and decomposition of the anhydrous citrate complex and free citric acid, through intermediates to the respective metal oxides [22]. The detailed analysis of TGA trace revealed the weight loss in step-1 as 2.61%. This could be due to the decomposition of trapped water molecules. It is apparent from Fig. 3, the decomposition of anhydrous citrate precursor started at 160 °C and hence the weight loss prior to the temperature 160 °C could be due to the trapped water molecules. Step-2 corresponds to the decomposition of intermediate phases such as aconitate, itaconic and other phases leading to the respective metal oxides [22], which is calculated as 2.62%. Step-3 corresponds to the decomposition of oxycarbonate compound, which was found to be stable up to 440 °C and then it decomposed at 490 °C. The meta-stable Co_2C and Co_3C phases also decomposed at 490 °C [23], accompanied by a weight loss of 6.36% in this region. Step-4 evidently shows a weight loss of 7.63% that corresponds to the decomposition of Sm_2C_3. When these carbides (Sm_2C_3) are heated, they vaporize incongruently and form Sm_2C and metallic Sm [24,25]. Above 776 °C, weight losses are negligible. A total weight loss of 19.22% was observed, which is convincing and confirms the complete decomposition of all the non-metallic phases.

The FT-IR spectra of samples: SMC-1, SMC-2, SMC-3 and SMC-4 are shown in Fig. 4. The spectrum of the gel-precursor showed a broad band around 3400 cm^{-1} indicates the O-H stretching due to the trapped water. The intensity of this band decreased when the sample was annealed to higher temperatures. A sharp peak around 1600 cm^{-1} is due to the C=O stretching indicating the presence of carboxylic group. The low intensity peaks at 2922, 2855 and 1316 cm^{-1} are due to the C-H stretching of alkanes [26]. Two sharp peaks that appear at 669 and 573 cm^{-1} in the spectrum of SMC-1 might be due to the result of metal-oxide vibrations [27] and these two low intensity peaks are also observed in all other spectra as well.

The FE-SEM image of the sample (SMC-2) obtained after reductive annealing at 350 °C is shown in Fig. 5. From the figure, it can be seen that the sample comprised in the form of

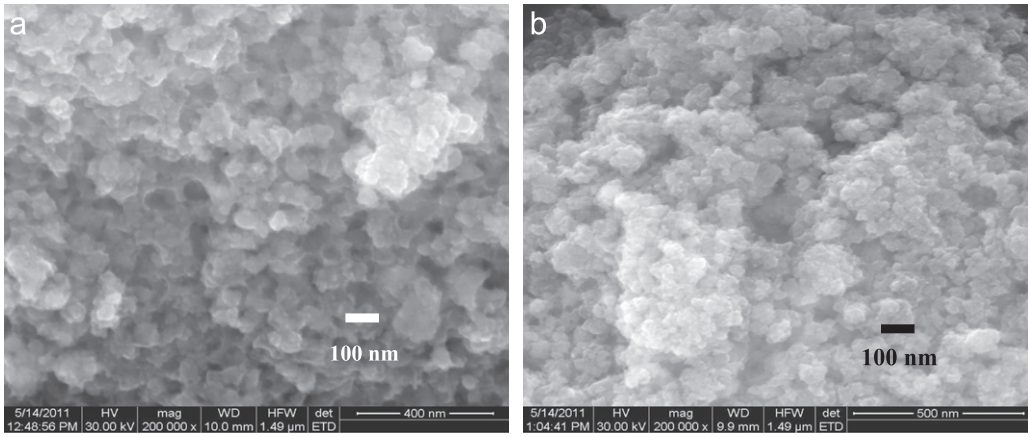

Fig. 6. FE-SEM images of samples: (a) SMC-3 and (b) SMC-4.

spherical granules with sizes in the range of sub-100 nm. The spherical granular nature of the sample is due to the dipolar interaction of the nanoparticles apart from the enormous surface energy [28]. Fig. 6 (a) and (b) shows the FE-SEM images of SMC-3 and SMC-4, respectively. Both the micrographs reveal agglomerated particles with irregular shapes due to the annealing of samples at sufficiently higher temperatures (500 and 600 °C). The carbonaceous coating from the citrate molecules stabilized the nanoparticles. When the sample coated with carbon subjected to annealing, the carbon coating decomposes and induces the particles to grow into irregular shapes and the above fact is witnessed in the FE-SEM images of the samples (Fig. 6(a) and (b)). EDX analysis was carried out to determine the elemental composition of the samples and the results are tabulated in Table 1.

The magnetic measurement of all the samples was carried out at room temperature and the typical M-H curves are shown in Fig. 7(a). All the samples demonstrated ferromagnetic behavior irrespective of their annealing conditions. Table 2 lists the magnetic properties of the four samples. From Fig. 7(b) of SMC-1, it could be observed that the saturation magnetization (M_s) of SMC-1 is very low (2.2 emu/g) due to the existence of oxide (Co_3O_4) phase, which is apparent from the XRD pattern (Fig. 1) and the coercivity (H_c) was found to be 1224 Oe, which is quite high among all the samples. The XRD pattern of SMC-1 can be indexed with the Co_3O_4 phase, which is an antiferromagnetic material. The Neel temperature (T_N) of Co_3O_4 is close to room temperature and it is a size dependent property. Despite the fact that weak ferromagnetism has been reported in the case of Co_3O_4 nanoparticles [29]; the observed moderate ferromagnetic behavior for the sample SMC-1 obtained in the present study could be due to the following facts: (i) finite size effects [30,31] and (ii) the presence of carbide and other Sm-Co phases in the samples. Although such phases are not seen in the XRD patterns and it is expected that these phases may be present in the amorphous form [32,33]. The M_s and H_c of SMC-2 are found to be 23.7 emu/g and 905 Oe, respectively. The observed increase in M_s could be due to the coexistence of Co_3O_4 along with the Co_xC (x=2, 3) phases. The H_c of SMC-2 is found to decrease when compared to SMC-1, which could be due to the existence of soft magnetic cobalt carbide phases (i.e. Co_3C) [12]. The M_s and H_c of SMC-3 were 39.3 emu/g and 1193 Oe respectively and these values were found to increase when compared to SMC-2, which was due to the maximum decomposition of Co_3O_4 phase and the crystallization of $SmCo_5$ alloy. This can be observed from the XRD pattern of SMC-3 (Fig. 2(a)). The decomposition of Co_3O_4 phase could be understood from the decrease in oxygen content (Table 1) of the EDX spectra (spectra not shown). The M_s and H_c of SMC-4 reached 100.2 emu/g and 1091 Oe, respectively, implies that the sample exhibits metallic Co, which is confirmed with the XRD analysis (Fig. 2(b)). The observed M_s (101 emu/g) coincides with the reported value [34], which is due to the existence of fcc-Co, as observed in the XRD pattern. The enhanced value of H_c (1091 Oe) might be due to the presence of cobalt carbide and the traces of amorphous Sm-Co. The crystallization of fcc-Co and Sm_2C_3 phases induces decomposition of $SmCo_5$ phase [25]. The controlled crystallization of Co and Sm_2C_3 phases such as those obtained in the present study will eventually drive the facile sol-gel technique to synthesize Sm-Co nanoparticles in large scale.

4. Conclusions

Although more work is needed to attain the expected Sm-Co crystallographic phase, our results are convincing for the

Table 1
Elemental composition of samples calculated using EDX.

Sample ID	Sm (wt %)	Co (wt %)	O (wt %)	C (wt %)
SMC-1	21.21	45.53	27.86	5.37
SMC-2	19.2	48.97	22.93	8.9
SMC-3	27.56	62.63	4.43	5.39
SMC-4	30.99	60.04	4.22	4.74

Table 2
Magnetic properties of samples prepared at various annealing conditions.

Sample Id	M_s (emu/g)	H_c (Oe)	M_r (emu/g)	Squareness ratio (M_r/M_s)
SMC-1	2.2	1224	1.0	0.47
SMC-2	23.7	905	9.5	0.40
SMC-3	39.3	1193	18.4	0.47
SMC-4	100.2	1091	40.2	0.40

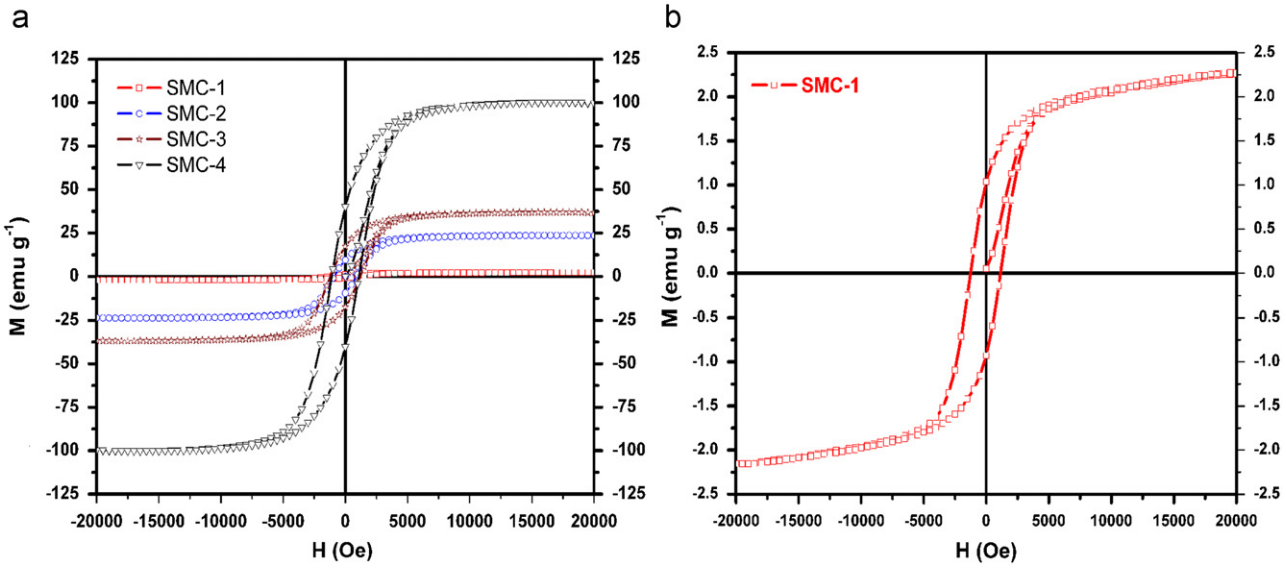

Fig. 7. (a) M-H loop of samples annealed at different temperatures and (b) M-H loop of SMC-1.

synthesis of Sm-Co alloy nanoparticles obtained through the facile sol-gel process. The major difficulty faced in the present work was the control of oxidation of metals and consecutive removal of oxides to achieve alloy nanoparticles. The existence of $SmCo_5$ phase is witnessed only in the case of SMC-3 sample. The sample annealed at 600 °C, induces crystallization of fcc-Co and Sm_2C_3 which deteriorated the $SmCo_5$ crystallographic phase completely. All the synthesized samples showed room temperature ferromagnetic behavior. The control of oxidation and growth of fcc-Co by modifying the existing synthesis protocols may trigger a new path way for the large-scale synthesis of nanoparticles of Sm-Co alloys towards fabrication of nanostructured hard magnets for sophisticated applications.

Acknowledgments

Authors G.S. and D.R.B. thank VIT University for the financial support, G.S. acknowledges the VIT University for the Research Associateship offered to him.

References

[1] O. Gutfleisch, Rare Earth Magnets: Materials, in: K.H.J. Buschow (Ed.), Concise Encyclopedia of Magnetic & Superconducting Materials, 2nd Edition,Elsevier Ltd., Oxford, 2005, pp. 1083–1086.
[2] O. Gutfleisch, High-Temperature Samarium Cobalt Permanent Magnets, in: J.Ping Liu, et al.et al.(Eds.), Nanoscale Magnetic Materials and Applications, Springer, New York, 2009, pp. 337–372.
[3] Y. Khan, A Contribution to the Sm-Co Phase Diagram, Acta Crystallographica B 30 (1974) 861–863.
[4] G.C. Hadjipanayis, Magnets: High-temperature, in: K.H.J. Buschow (Ed.), Concise Encyclopedia of Magnetic and Superconducting Materials, 2nd Edition, Elsevier Ltd., Oxford, 2005, pp. 866–870.
[5] Y. Hou, Zhichuan Xu, Sheng Peng, J.Ping Chuanbing Rong, Liu, and Shouheng Sun, A Facile Synthesis of SmCo5 Magnets from Core/Shell Co/Sm2O3 Nanoparticles, Advanced Materials (Weinheim, Germany) 19 (2007) 3349–3352.
[6] Y. Wang, Yang Li, Chuan bing Rong and J Ping Liu, Sm-Co hard magnetic nanoparticles prepared by surfactant-assisted ball milling, Nanotechnology 18 (2007) 465701.
[7] G.S. Chaubey, Narayan Poudyal, Yuzi Liu, Chuanbing Rong, J. Ping Liu, Synthesis of Sm-Co and Sm-Co/Fe nanocrystals by reductive annealing of Nanoparticles, Journal of Alloys and Compounds 509 (2011) 2132–2136.
[8] T. Matsushita, Takashi Iwamoto, Makoto Inokuchi, Naoki Toshima, Novel ferromagnetic materials of SmCo5 nanoparticles in single-nanometer size: chemical syntheses and characterizations, Nanotechnology 21 (2010) 095603.
[9] P. Saravanan, G. Venkata Ramana, K. Srinivasa Rao, B. Sreedhar, V.T.P. Vinod, V. Chandrasekaran, Structural and magnetic properties of self-assembled Sm–Co spherical aggregates, Journal of Magnetism and Magnetic Materials 323 (2011) 2083–2089.
[10] P. Saravanan, G. Venkata Ramana, K. Srinivasa Rao, B. Sreedhar, A. Perumal, Thin magnetic films of Sm–Co nanocrystallites exploiting spin coating deposition, Thin Solid Films 519 (2011) 6290–6296.
[11] P. Saravanan, K. Srinivasa Rao, D. Mishra, A. Perumal, V. Chandrasekaran, One-Step Synthesis of Sm-Co Spherical Granules via Superhydride Reduction, Advanced Science Letters 3 (2010) 49–52.
[12] V.G. Harris, Y. Chen, A. Yang, S. Yoon, Z. Chen, A.L. Geiler, J. Gao, C.N. Chinnasamy, L.H. Lewis, C. Vittoria, E.E. Carpenter, K.J. Carroll, R. Goswami, M.A. Willard, L. Kurihara, M. Gjoka, O. Kalogirou, High coercivity cobalt carbide nanoparticles processed via polyol reaction: a new permanent magnet material, Journal of Physics D: Applied Physics 43 (2010) 165003.
[13] C.N. Chinnasamy, J.Y. Huang, L.H. Lewis, B. Latha, C. Vittoria, V.G. Harris, Direct chemical synthesis of high coercivity air-stable SmCo nanoblades, Applied Physics Letters 93 (2008) 032505.
[14] C.N. Chinnasamy, J.Y. Huang, L.H. Lewis, C. Vittoria, V.G. Harris, Erratum: Direct chemical synthesis of high coercivity SmCo nanoblades, Applied Physics Letters 93 (2008) 032505. Applied Physics Letters 97 (2010) 059901.
[15] C. Liu, Xiaowei Wu, Timothy Klemmer, Nisha Shukla, Xiaomin Yang, Dieter Weller, Anup G. Roy, Mihaela Tanase and David Laughlin, Polyol Process Synthesis of Monodispersed FePt Nanoparticles, The Journal of Physical Chemistry B 108 (2004) 6121–6123.
[16] Petr Vanýsek, Electrochemical Series, in: David R. Lide (Ed.), CRC Handbook of Chemistry and Physics, 87th Edition,Taylor and Francis, Boca Raton, FL, 2007. 8–20-8–29.
[17] B.L. Cushing, Vladimir L. Kolesnichenko, Charles J. O'Connor, Recent Advances in the Liquid-Phase Syntheses of Inorganic Nanoparticles, Chemical Reviews 104 (2004) 3893–3946.
[18] C.B. Rong, D. Li, V. Nandwana, N. Poudyal, Y. Ding, Z.L. Wang, H. Zeng, J.P. Liu, Size-Dependent Chemical and Magnetic Ordering in L10-FePt Nanoparticles, Advanced Materials (Weinheim, Germany) 18 (2006) 2984–2988.
[19] W.S. Seo, Jin Hyung Lee, Xiaoming Sun, Yoriyasu Suzuki, Davidmann, Zhuang Liu, Masahiro Terashima, Philip C. Yang, Michael V. Mcconnell, Dwight G. Nishimura, Hongjie Dai, FeCo/graphitic-shell nanocrystals as advanced magnetic-resonance-imaging and near-infrared agents, Nature materials 5 (2006) 971–976.
[20] H. Wang, S.P. Wong, W.Y. Cheung, N. Ke, W.F. Lau, M.F. Chiah, X.X. Zhang, Structural and magnetic properties of Co65C35 nanocomposite films prepared by pulsed filtered vacuum arc deposition, Materials Science and Engineering, C: Materials for Biological Applications 16 (2001) 147–151.
[21] R.N. Panda, J.C. Shih, T.S. Chin, Magnetic properties of nano-crystalline Gd-or Prsubstituted CoFe2O4 synthesized by the citrate precursor technique, Journal of Magnetism and Magnetic Materials 257 (2003) 79–86.
[22] N.S. Gajbhiye, Seema Prasad, Thermal decomposition of hexahydrated nickel iron citrate, Thermochimica Acta 285 (1996) 325–336.
[23] Y. Zhang, Girija S. Chaubey, Chuanbing Rong, Yong Ding, Narayan Poudyal, Poching Tsai, Qiming Zhang, J. Ping Liu, Controlled synthesis and magnetic properties of hard magnetic CoxC (x=2, 3) nanocrystals, Journal of Magnetism and Magnetic Materials 323 (2011) 1495–1500.
[24] J.M. Haschke, Thomas A Deline, Vaporization and thermodynamic properties of samarium dicarbide and sub-stoichiometric disamarium tricarbide, Journal of Chemical Thermodynamics 14 (1982) 1019–1028.
[25] H.W. Chang, S.T. Huang, C.W. Chang, W.C. Chang, A.C. Sun, Y.D. Yao, Effect of C addition on the magnetic properties, phase evolution, and microstructure of melt spun $SmCo_{7-x}Hf_x$ (x=0.1–0.3) ribbons, Solid State Communications 147 (2008) 69–73.
[26] P.K. Deheri, Viswanathan Swaminathan, Shekhar D. Bhame, Zhongwu Liu, Raju V. Ramanujan, Sol-Gel Based Chemical Synthesis of $Nd_2Fe_{14}B$ Hard Magnetic Nanoparticles, Chemistry of Materials : A Publication of the American Chemical Society 22 (2010). 6509-6417.
[27] J. Jiu, Yue Ge, Xiaoning Li, Ling Nie, Preparation of Co_3O_4 nanoparticles by a polymer combustion route, Materials Letters 54 (2002) 260–263.
[28] X.W. Wei, Guo-Xing Zhu, Yuan-Jun Liu, Yong-Hong Ni, You Song, Zheng Xu, Large-Scale Controlled Synthesis of FeCo Nanocubes and Microcages by Wet chemistry, Chemistry of Materials : A Publication of the American Chemical Society 20 (2008) 6248–6253.
[29] A. Tomou, D. Gournis, I. Panagiotopoulos, Y. Huang, G.C. Hadjipanayis, B.J. Kooi, Weak ferromagnetism and exchange biasing in cobalt oxide nanoparticle systems, Journal of Applied Physics 99 (2006) 123915.
[30] X. Batlle, Amílcar Labarta, Finite-size effects in fine particles: magnetic and transport properties, Journal of Physics D: Applied Physics 35 (2002) R15–R42.
[31] R.H. Kodama, Salah A. Makhlouf, A.E. Berkowitz, Finite Size Effects in Antiferromagnetic NiO Nanoparticles, Physical Review Letters 79 (1997) 1393–1396.
[32] C.D. Graham Jr., T. Egami, Magnetic Properties of Amorphous Alloys, Annual Review of Materials Science 8 (1978) 423–457.
[33] D.L. Leslie-Pelecky, R.L. Schalek, Effect of disorder on the magnetic properties of SmCo5, Physical Review B 59 (1999) 457–462.
[34] R.N. Grass, Wendelin J. Stark, Gas phase synthesis of fcc-cobalt nanoparticles, Journal of Materials Chemistry 16 (2006) 1825–1830.